Mechanisms of high-order photobleaching and its relationship to intracellular ablation

S. Kalies,* K. Kuetemeyer, and A. Heisterkamp

Laser Zentrum Hannover e.V., Hollerithallee 8, 30419 Hannover, Germany

* s.kalies@lzh.de

Abstract: In two-photon laser-scanning microscopy using femtosecond laser pulses, the dependence of the photobleaching rate on excitation power may have a quadratic, cubic or even biquadratic order. To date, there are still many open questions concerning this so-called *high-order photobleaching*. We studied the photobleaching kinetics of an intrinsic (enhanced Green Fluorescent Protein (*eGFP*)) and an extrinsic (Hoechst 33342) fluorophore in a cellular environment in two-photon microscopy. Furthermore, we examined the correlation between bleaching and the formation of reactive oxygen species. We observed bleaching-orders of three and four for eGFP and two and three for Hoechst increasing step-wise at a certain wavelength. An increase of reactive oxygen species correlating with the bleaching over time was recognized. Comparing our results to the mechanisms involved in intracellular ablation with respect to the amount of interacting photons and involved energetic states, we found that a low-density plasma is formed in both cases with a smooth transition in between. Photobleaching, however, is mediated by sequential-absorption and multiphoton-ionization, while ablation is dominated by the latter and cascade-ionization processes.

OCIS codes: (170.3880) Medical and biological imaging; (180.4315) Nonlinear microscopy; (190.4180) Multiphoton processes; (170.1020) Ablation of tissue.

References and links

1. W. Denk, J. H. Strickler, and W. W. Webb, "Two-photon laser scanning fluorescence microscopy," Science **248**, 73–76 (1990).
2. W. Denk and K. Svoboda, "Photon upmanship: why multiphoton imaging is more than a gimmick," Neuron **18**, 351–357 (1997).
3. S. W. Hell and J. Wichmann, "Breaking the diffraction resolution limit by stimulated emission: stimulated-emission-depletion fluorescence microscopy," Opt. Lett. **19**, 780–782 (1994).
4. T. Hirschfeld, "Quantum efficiency independence of the time integrated emission from a fluorescent molecule," Appl. Opt. **15**, 3135–3139 (1976).
5. L. Song, E. J. Hennink, I. T. Young, and H. J. Tanke, "Photobleaching kinetics of fluorescein in quantitative fluorescence microscopy," Biophys. J. **68**, 2588–2600 (1995).
6. L. Song, C. A. Varma, J. W. Verhoeven, and H. J. Tanke, "Influence of the triplet excited state on the photobleaching kinetics of fluorescein in microscopy," Biophys. J. **70**, 2959–2968 (1996).
7. C. Eggeling, J. Widengren, R. Rigler, and C. A. M. Seidel, "Photobleaching of Fluorescent Dyes under Conditions Used for Single-Molecule Detection: Evidence of Two-Step Photolysis," Anal. Chem. **70**, 2651–2659 (1998).
8. C. Eggeling, A. Volkmer, and C. A. M. Seidel, "Molecular photobleaching kinetics of Rhodamine 6G by one- and two-photon induced confocal fluorescence microscopy," ChemPhysChem **6**, 791–804 (2005).
9. V. Kasche and L. Lindqvist, "Reactions between the Triplet State of Fluorescein and Oxygen," J. Chem. Phys. **68**, 817–823 (1964).

#141169 - $15.00 USD Received 14 Jan 2011; revised 18 Feb 2011; accepted 20 Feb 2011; published 4 Mar 2011

10. G. H. Patterson and D. W. Piston, "Photobleaching in two-photon excitation microscopy," Biophys. J. **78**, 2159–2162 (2000).
11. T.-S. Chen, S.-Q. Zeng, Q.-M. Luo, Z.-H. Zhang, and W. Zhou, "High-order photobleaching of green fluorescent protein inside live cells in two-photon excitation microscopy," Biochem. Biophys. Res. Commun. **291**, 1272–1275 (2002).
12. T. Chen, Z. W. Zeng, SQ, and Q. Luo, "A Quantitative Theory Model of a Photobleaching Mechanism," Chinese Phys. Lett. **20**, 1940 (2003).
13. A. Reuther, D. N. Nikogosyan, and A. Laubereau, "Primary Photochemical Processes in Thymine in Concentrated Aqueous Solution Studied by Femtosecond UV Spectroscopy," J. Chem. Phys. **100**, 5570–5577 (1996).
14. P. S. Dittrich and P. Schwille, "Photobleaching and stabilization of fluorophores used for single-molecule analysis with one- and two-photon excitation," Appl. Phys. B **73**, 829–837 (2001).
15. K. Koenig, I. Riemann, P. Fischer, and K. J. Halbhuber, "Intracellular nanosurgery with near infrared femtosecond laser pulses," Cell. Mol. Biol. **45**, 195–201 (1999).
16. A. Vogel, J. Noack, G. Huettman, and G. Paltauf, "Mechanisms of femtosecond laser nanosurgery of cells and tissues," Appl. Phys. B **81**, 1015–1047 (2005).
17. P. A. Quinto-Su and V. Venugopalan, "Mechanisms of laser cellular microsurgery," Methods Cell Biol. **82**, 113–151 (2007).
18. B. Boudaiffa, P. Cloutier, D. Hunting, M. A. Huels, and L. Sanche, "Resonant formation of DNA strand breaks by low-energy (3 to 20 eV) electrons," Science **287**, 1658–1660 (2000).
19. L. Sanche, "Low energy electron-driven damage in biomolecules," Eur. Phys. D **35**, 367–390 (2005).
20. U. K. Tirlapur, K. Koenig, C. Peuckert, R. Krieg, and K. J. Halbhuber, "Femtosecond near-infrared laser pulses elicit generation of reactive oxygen species in mammalian cells leading to apoptosis-like death," Exp. Cell Res. **263**, 88–97 (2001).
21. B. P. Yu, "Cellular Defenses Against Damage From Reactive Oxygen Species," Physiol. Rev. **75** (1995).
22. K. Kuetemeyer, R. Rezgui, H. Lubatschowski, and A. Heisterkamp, "Influence of laser parameters and staining on femtosecond laser-based intracellular nanosurgery," Biomed. Opt. Express **1**, 587–597 (2010).
23. A. Heisterkamp, J. Baumgart, I. Z. Maxwell, A. Ngezahayo, E. Mazur, and H. Lubatschowski, "Fs-laser scissors for photobleaching, ablation in fixed samples and living cells, and studies of cell mechanics," Methods Cell Biol. **82**, 293–307 (2007).
24. I. Gryczynski and J. R. Lakowicz, "Fluorescence intensity and anisotropy decays of the DNA stain Hoechst 33342 resulting from one-photon and two-photon excitation," J. Fluoresc. **4**, 331–336 (1994).
25. A. A. Heikal, S. T. Hess, and W. W. Webb, "Multiphoton molecular spectroscopy and excited-state dynamics of enhanced green fluorescent protein (EGFP): acid-base specificity," Chem. Phys. **274**, 37–55 (2001).
26. M. Vengris, I. H. van Stokkum, X. He, A. F. Bell, P. J. Tonge, R. van Grondelle, and D. S. Larsen, "Ultrafast excited and ground-state dynamics of the green fluorescent protein chromophore in solution," J. Phys. Chem. A **108**, 4587–4598 (2004).
27. E. Epifanovsky, I. Polyakov, B. Grigorenko, A. Nemukhin, and A. I. Krylov, "The effect of oxidation on the electronic structure of the green fluorescent protein chromophore," J. Chem. Phys. **132**, 115104 (2010).
28. M. Ormo, A. B. Cubitt, K. Kallio, L. A. Gross, R. Y. Tsien, and S. J. Remington, "Crystal structure of the Aequorea victoria green fluorescent protein," Science **273**, 1392–1395 (1996).
29. E. Amouyal, A. Bernas, and D. Grand, "On the photoionization energy threshold of tryptophan in aqueous solutions," Photochem. Photobiol. **29**, 1071–1077 (1979).
30. R. H. Bisby, A. G. Crisostomo, S. W. Botchway, and A. W. Parker, "Nanoscale hydroxyl radical generation from multiphoton ionization of tryptophan," Photochem. Photobiol. **85**, 353–357 (2009).
31. F. Bourgeois and A. Ben-Yakar, "Femtosecond laser nanoaxotomy properties and their effect on axonal recovery in C. elegans," Opt. Express **15**, 8521–8531 (2007).
32. K. K. Kalninsh, D. V. Pestov, and Y. K. Roshchina, "Absorption and fluorescence spectra of the probe Hoechst 33258," J. Photochem. Photobiol. A: Chem. **83**, 39–47 (1994).
33. H. Goerner, "Direct and sensitized photoprocesses of bis-benzimidazole dyes and the effects of surfactants and DNA," Photochem. Photobiol. **73**, 339–348 (2001).
34. E. Olmo, "Nucleotype and cell size in vertebrates: a review," Basic Appl Histochem **27**, 227–256 (1983).
35. F. G. Loontiens, P. Regenfuss, A. Zechel, L. Dumortier, and R. M. Clegg, "Binding characteristics of hoechst 33258 with calf thymus dna, poly[d(a-t)], and d(ccggaattccgg): multiple stoichiometries and determination of tight binding with a wide spectrum of site affinities," Biochemistry **29**, 9029–9039 (1990).
36. I. D. Johnson, "Practical considerations in the selection and application of fluorescent probes," in "Handbook of Biological Confocal Microscopy," J. B. Pawley, ed. (Springer, 2006).

#141169 - $15.00 USD Received 14 Jan 2011; revised 18 Feb 2011; accepted 20 Feb 2011; published 4 Mar 2011

1. Introduction

Over the past twenty years, microscopy was revolutionized by the use of non-linear optical phenomena establishing new highly reliable fluorescence imaging methods. These have certain advantages in contrast to conventional confocal laser-scanning microscopy. Two-photon based microscopy introduced by Denk et al. [1] broke into new areas of deep tissue and cellular imaging [2]. The use of near-infrared wavelengths results in an increased penetration depth up to 1 mm and reduced scattering effects, because of missing endogenous absorbers in this wavelength range. Furthermore, nonlinear absorption is limited to the focal volume [1]. Other techniques, like STED by Hell et al. [3] opened up the possibility to improve the imaging resolution beyond the Abbe limit. Despite all this progress in imaging methods, a major problem remains: the lifetime of every fluorophore is limited by photochemical destruction, generally called photobleaching.

In photobleaching, a fluorophore loses its ability to emit light over several absorption- and emission-circles [4, 5]. The loss of fluorescence over time added up for all fluorophores in the focal volume has a multi-exponential form characterized by the photobleaching rate. Song et al. and Eggeling et al. did major work on explaining photobleaching of linear excitation [5–8]. In this case, the rate of photobleaching scales linearly with the power of excitation and bleaching is strongly influenced by the presence of molecular oxygen in the environment [5, 9]. The population of the first excited triplet state plays a key role, as a low triplet population results in low photobleaching [6]. Molecular oxygen in triplet state can further interact with the first triplet of the fluorophore in photooxidation and in this way form a nonfluorescent fluorophore-radical and singlet molecular oxygen [5].

In two-photon microscopy with ultra-short laser pulses, various experiments have reported higher order dependencies of the photobleaching rate on excitation power [8, 10–12]. For instance, Patterson et al. examined the photobleaching of several fluorophores and found an order of three [10], while Chen et al. even measured a fourth order for a mutant of the green fluorescent protein (GFP) [11]. Related to this, photobleaching in the focal volume is faster with nonlinear- than with linear-excitation. Hence, exhaustive knowledge should be gained to understand and avoid it. As significantly higher intensities are used in nonlinear microscopy [1], new photobleaching channels open up due to the possibility of sequential-excitation into higher electronic states than the first singlet or triplet [8]. In polar solvents like water, these states couple quite efficiently with ionic states [13]. This so-called photolysis has been readily observed with high power cw and pulsed lasers in two-photon confocal fluorescence microscopy for Rhodamine 6G dye by Eggeling et al. [8].

For fs-pulsed excitation, triplet population does not seem to be a key factor in photobleaching and two-step photolysis [8, 14]. In this case, an absorption in the first excited singlet state is likely immediately followed by another one-photon absorption in a higher state because of the huge photon density. These saturated transitions are negligible in the photobleaching-order [8]. Although extensive work has been done in the past years concerning high-order photobleaching, there are still many open questions. Up to date, to the best of our knowledge, it was not examined in a large wavelength range or at different repetition rates. Furthermore, a comparison of photobleaching to other laser-mediated processes in microscopy, like ablation, is not yet given in detail.

Since its first demonstration by Koenig et al. [15], femtosecond laser cell surgery has proven to be an excellent tool for non-invasive and precise manipulation of single cell organelles. In the so-called low-density plasma regime, several thousand and more pulses with pulse energies below the optical breakdown threshold and repetition rates around 80 MHz are used [16]. The created photon densities are sufficient to induce multiphoton-ionization in a sub-femtoliter volume. Together with cascade-ionization, very high free-electron densities are generated inducing

#141169 - $15.00 USD Received 14 Jan 2011; revised 18 Feb 2011; accepted 20 Feb 2011; published 4 Mar 2011

chemical decomposition (bond breaking) of biomolecules [16–19]. In addition, reactive oxygen species (ROS) are produced by multiphoton-ionization and dissociation of water molecules, such as the hydroxyl radical (OH-). ROS are known to react efficiently with biomolecules, such as DNA bases, and may induce cell death at high concentrations [20, 21]. One of the recent papers of our group revealed that these photochemical processes are finished within a few nanoseconds [22]. Accumulation over many pulses leads to ablation of biological material. Heisterkamp et al. found, that the ablation threshold is about 20% higher than the photobleaching threshold [23]. From this point of view, one can suggest that there is a smooth transition from high-order photobleaching to ablation.

In this study, we measured the photobleaching-order over a large wavelength range from 720 to 950 nm and two repetition rates at 4 and 80 MHz for two distinct fluorophores, eGFP and Hoechst. We analysed the differences of high-order photobleaching and ablation in view of involved photons and energetic levels. In addition, we measured the amount of produced reactive oxygen species in time-correlation with high-order photobleaching and tested its influence on other fluorophores in the focal volume. Furthermore, the effects of high-order photobleaching on cellular viability were examined.

2. Materials and methods

2.1. Laser system and image acquisition

The laser system is a Ti:sapphire laser (Chameleon Ultra II, Coherent) generating ultra-short pulses of 140 fs at a repetition rate of 80 MHz. The accessible wavelength ranges from 680 to 1080 nm with a mean power greater than 3.5 W. An acousto-optical pulse picker (Pulse Select, APE) regulates the repetition rate with a division ratio between 1:20 and 1:80000, corresponding to 4 MHz and 1 kHz. Only repetition rates of 80 MHz and 4 MHz were used in this study, as the average power at lower repetition rates was too low for photobleaching within a reasonable time of 10 min.

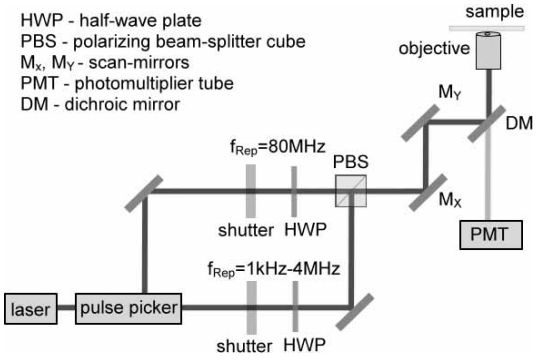

Fig. 1. Schematic set-up for multiphoton imaging and logging of photobleaching kinetics.

The diffracted and initial laser beam were guided through a mechanical shutter (Thorlabs, SC10) and an attenuator, consisting of a half-wave plate and a polarizing beam-splitter cube (see Fig. 1) and then superimposed. Two galvanometer scan-mirrors (Cambridge Technology) deflected both beams into the tubus of an inverted microscope (Axiovert 100, Carl Zeiss AG) via a dichroic mirror. Focussing into the sample was done by a 1.3-NA oil immersion objective (Plan-Neofluar, Carl Zeiss AG) or a 0.85-NA water immersion objective (C-Achroplan, Carl Zeiss AG). The fluorescence, which returned through the objective and the dichroic mirror, was detected by a photomultiplier tube (R6357, Hamamatsu Photonics).

#141169 - $15.00 USD Received 14 Jan 2011; revised 18 Feb 2011; accepted 20 Feb 2011; published 4 Mar 2011

2.2. Cell cultures and labelling

Photobleaching experiments with the fluorophore Hoechst 33342 (Invitrogen, emission: 461 nm, bandpass-filter: 475 ± 21 nm) were done with bovine capillary endothelial cells. The cells were cultivated in plastic bottom dishes with a thickness of 180 μm (ibidi GmbH) using RPMI 1640 medium (Roswell Park Memorial Institute) supplemented with 10% fetal calf serum (FCS) and the antibiotics penicillin and streptomycin at 37 °C and 5% humidified CO_2 atmosphere. For staining of nuclear DNA with Hoechst, cells were incubated for 10 min at 37 °C with a final concentration of 2 μg/mL in RPMI medium. Then, they were washed two times. The eGFP (emission: 509 nm, bandpass-filter: 525 ± 25 nm) expressing RAT1 cells (mouse fibroblasts) were cultivated in plastic bottom dishes using DMEM medium (Dulbecco's Modified Eagle Medium) with the same supplements and under the same conditions. As eGFP is expressed by protein biosynthesis, no further staining was necessary.

To measure the oxidative stress, bovine endothelial cells were first stained with Hoechst as described above and then incubated for 20 min with 5 μM of the ROS indicator 2,7-dichlorodihydrofluorescein diacetate (CM-H2DCFDA, Invitrogen, emission: 525 nm, bandpass-filter: 525 ± 25 nm) in NaCl medium. Next, the cells were washed two times and NaCl medium was replaced with RPMI medium. After cellular uptake, the non-fluorescent 2,7-dichlorodihydrofluorescein diacetate is cleaved by cellular esterases and then oxidized by ROS to the fluorescent form 2,7-dichlorofluorescein.

For the evaluation of cell viability, Hoechst stained photobleached cells were co-stained with Propidium Iodide (Invitrogen, emission: 617 nm, final concentration: 15 μM, bandpass-filter: 655 ± 20 nm) and Calcein AM (Invitrogen, emission: 515 nm, final concentration: 20 μM, bandpass-filter: 525 ± 25 nm) thirty minutes after bleaching with an incubation time of 15 min. The plastic bottom dishes were placed into a microscope stage incubation system (Okolab), which was set to 37 °C and 5% CO_2 humidified atmosphere. The acetomethoxy group of the membrane permeable Calcein AM is removed by cellular esterases in live cells, making Calcein green fluorescent. Propidium Iodide only binds to nuclear DNA, if the plasma membrane integrity is lost, as in necrotic cells.

To evaluate the influence of fluorophore photobleaching on its environment, RAT1 cells were stained with Hoechst. The cells were incubated for 10 min at 37 °C with a Hoechst concentration of 2 μg/mL in DMEM medium.

2.3. Logging of fluorescence properties and photobleaching kinetics

To measure the amount of absorbed photons per excitation event (multiphoton-order) in a regime with no recognizable photobleaching, fluorescence intensity I versus mean power P was recorded for several powers at the same position of the sample. The obtained data was fitted exponentially, giving the resulting multiphoton-order x_{mp} as exponent: $I = \text{const.} \cdot P^{x_{mp}}$.

In photobleaching experiments the sample was raster-scanned in a meandering way. The fluorescence intensity was logged over time with a temporal resolution of about 150 ms. To obtain the order of photobleaching x_{bleach}, the half-life period $t_{1/2}$ of the fluorophores in the focal volume was noticed for different powers. This is the time, in which half of the initial fluorophores were bleached. Bleaching could be well described by a single exponential function $N(t) = N_0 \cdot \exp(-k \cdot t)$ in this study, with $N(t)$ and N_0 being the amount of remaining and initial fluorescent dyes, being bleached over a time t with a rate k. Therefore, the half-life period is reciprocal to k with a factor $\ln(2)$. As the photobleaching rate also depends on mean power with the photobleaching order x_{bleach} as scaling exponent ($k = \ln(2)/t_{1/2} = \text{const.} \cdot P^{x_{bleach}}$), this order can be gained by fitting the half-life period exponentially against multiple mean powers.

To evaluate the influence of fluorophore photobleaching on its environment using Hoechst stained RAT1 cells, two different wavelengths, 720 and 900 nm were used to distinguish be-

#141169 - $15.00 USD Received 14 Jan 2011; revised 18 Feb 2011; accepted 20 Feb 2011; published 4 Mar 2011

tween the fluorescence signals of eGFP and Hoechst. While Hoechst has a large absorption cross-section at the minor wavelength, this is reversed for eGFP. Bleaching and fluorescence intensity measurement of eGFP was done at 900 nm, while Hoechst fluorescence was measured at 720 nm. As Hoechst as well as eGFP were invisible in the detected fluorescence signal at 900 and 720 nm, respectively, direct photobleaching of Hoechst most likely did not occur. To underline this, the half-life periods with and without the addition of Hoechst were compared and found to be equal.

For the measurement of oxidative stress, bleaching of Hoechst and excitation of 2,7-dichlorofluorescein were simultaneously done at a wavelength of 860 nm. The fluorescence intensity of 2,7-dichlorofluorescein was logged. The exponential decay of the Hoechst fluorescence due to photobleaching was modelled afterwards by the measured half-life period for these parameters.

Test of statistical significance were done using Sigmastat 3.5 (Systat Software GmbH) while Origin 8.5 (OriginLab) was used for plotting and nonlinear regression. Differences between data points were considered significant at $P \leq 0.05$.

3. Results

3.1. Multiphoton- and photobleaching-orders of Hoechst and eGFP

Irradiation of Hoechst stained endothelial cells with mean powers well below the photobleaching threshold led to an almost quadratic increase of fluorescence intensity versus mean power in the wavelength range of 720 up to 800 nm (see Fig. 2). Between 850 and 950 nm the multiphoton-order increased to values within two and three. A significant difference between the data points of both wavelength ranges was revealed by an ANOVA and a Tukey-test ($P \leq 0.001$). Therefore, two-photon absorption dominated at the lower wavelengths, while three-photon absorption became more likely above 850 nm.

For eGFP the multiphoton-order yielded a value of approximately two over the whole wavelength range (see Fig. 2) according to two-photon excitation. Below 800 nm, there also was weak one-photon absorption, giving multiphoton-orders slightly below two. However, this difference was not statistically significant ($P > 0.12$, ANOVA and Tukey-test).

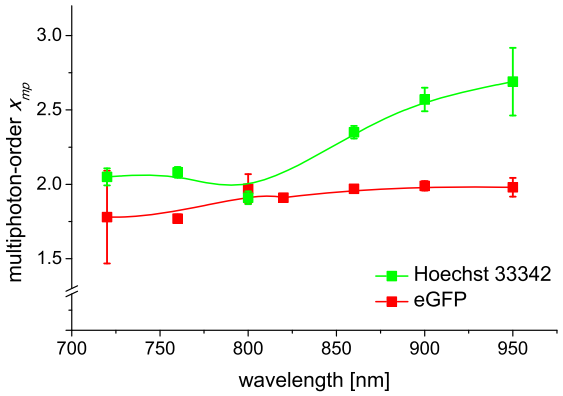

Fig. 2. Wavelength-dependence of the multiphoton-order for Hoechst 33342 and eGFP. Each data point represents the mean ± standard deviation of at least five experiments. The multiphoton-order was about two over the whole wavelength range for eGFP, while it increased from two up to three for Hoechst.

#141169 - $15.00 USD Received 14 Jan 2011; revised 18 Feb 2011; accepted 20 Feb 2011; published 4 Mar 2011

In photobleaching of eGFP, we obtained bleaching-orders of approximately three from 720 up to 800 nm (see Fig. 3) with no significant difference between these data points ($P = 0.07$, ANOVA). A sudden significant increase of the bleaching-order by one occurred at a wavelength of circa 840 nm ($P < 0.001$, ANOVA and Tukey-test). From 860 to 920 nm, the bleaching-orders varied slightly around four. Excluding the anomaly of the photobleaching-order gained by the measurements at 920 nm, 4 MHz and NA 1.3, there was no significant difference between these data points ($P = 0.37$, ANOVA).

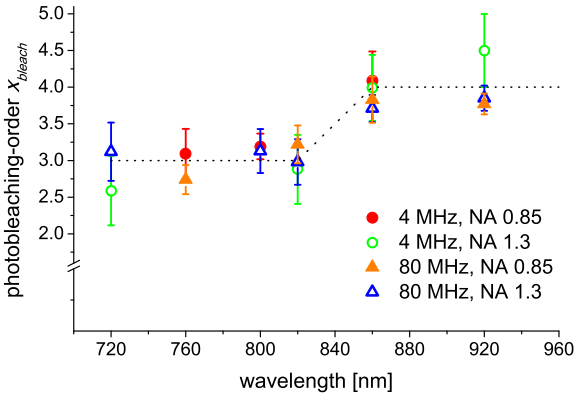

Fig. 3. Wavelength-dependence of the photobleaching-order for eGFP at different laser-parameters. The dotted line illustrates its behaviour. Each data point represents the mean ± standard deviation of at least five experiments. While the photobleaching-order was independent of repetition rate and NA, there was a step increase of one at about 840 nm.

For Hoechst we obtained similar results as for eGFP with bleaching orders around two. A significant step increase by one was located at approximately 930 nm (see Fig. 4) ($P \leq 0.001$, ANOVA and Tukey-test). By contrast , the photobleaching-order was independent of the laser wavelength below 920 nm ($P \geq 0.06$, ANOVA).

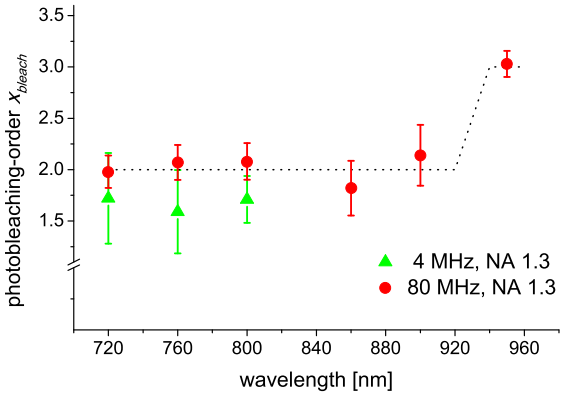

Fig. 4. Wavelength-dependence of the photobleaching-order for Hoechst at different repetition rates. The dotted line illustrates its behaviour. Each data point represents the mean ± standard deviation of at least five experiments. The bleaching-order varied slightly around two from 720 up to 900 nm and increased to three at 950 nm.

Following the results of the statistical test, the repetition rate and numerical aperture had no

#141169 - $15.00 USD Received 14 Jan 2011; revised 18 Feb 2011; accepted 20 Feb 2011; published 4 Mar 2011

significant influence on the photobleaching-order for both dyes at all wavelengths.

3.2. Formation of reactive oxygen species and influence of photobleaching on its environment

We found an increase of reactive oxygen species (ROS) in the cellular environment over time while we photobleached Hoechst (see Fig. 5(a)). It saturated at the same point, were photobleaching had destroyed almost every fluorophore (see Fig. 5(b)). Furthermore, a direct correlation was given, as the half-life period of photobleaching and the half-saturation value of ROS formation were approximately at the same time. This behaviour was found for several mean powers, equal to different half-life periods ($P \geq 0.08$, ANOVA).

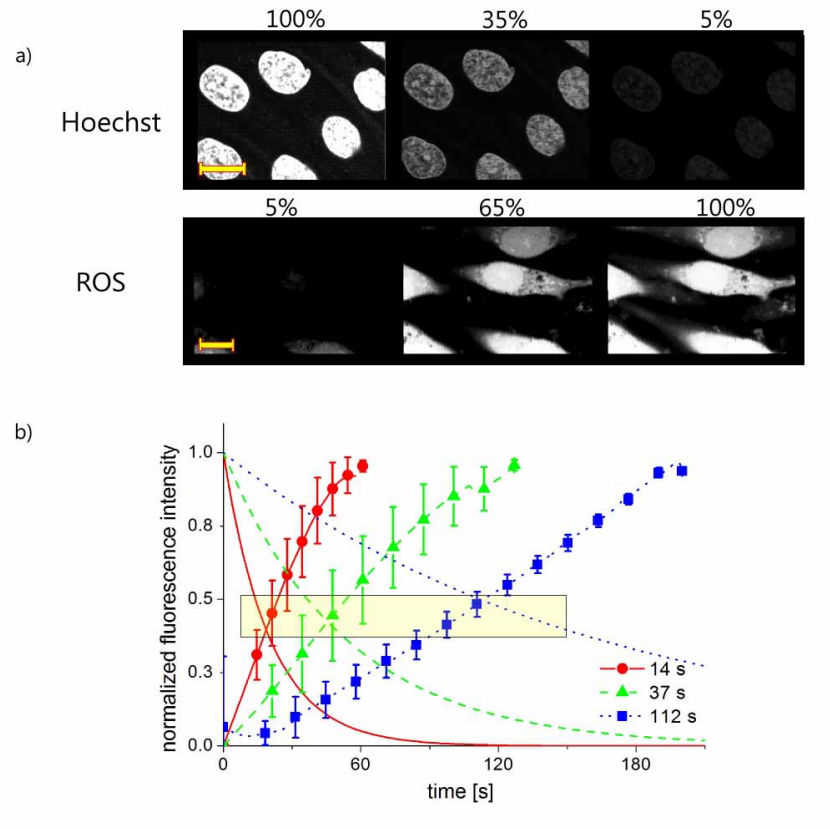

Fig. 5. Correlation of ROS formation and high-order photobleaching. (a) Multiphoton images from different points of time during photobleaching. ROS concentration increased during the drop in Hoechst fluorescence. Scale bar: 8 μm. (b) Time-dependence of ROS formation in comparison to Hoechst photobleaching for three half-life periods. Each data point represents the mean $\pm$ standard deviation of at least five cells. The half-life period of photobleaching and the half-saturation value of ROS formation were approximately at the same time (yellow box).

A live-dead assay with the fluorophores calcein and propidium iodide in photobleached and Hoechst stained endothelial cells showed no influence of photobleaching on cell viability, as calcein was fluorescent while propidium iodide was not. In addition, we observed the eGFP expressing RAT1 cells for several hours after bleaching and found a recovery of eGFP fluorescence resulting from the formation of new eGFP. Furthermore, cell division was found to be intact (data not shown).

#141169 - $15.00 USD Received 14 Jan 2011; revised 18 Feb 2011; accepted 20 Feb 2011; published 4 Mar 2011

Photobleaching of eGFP at a wavelength of 900 nm in Hoechst stained RAT1 cells provided an intensity loss of about 50-80% in the Hoechst fluorescence signal at 720 nm referred to an absolute bleaching of eGFP (see Fig. 6). This behaviour was independent of the half-life period and repetition rate ($P = 0.65$, ANOVA). Furthermore, no significant difference of the half-life periods with and without the addition of Hoechst was found (data not shown, $P \geq 0.08$, t-test for each power) suggesting that bleaching of Hoechst is not related to a direct Hoechst-fluorophore - photon interaction.

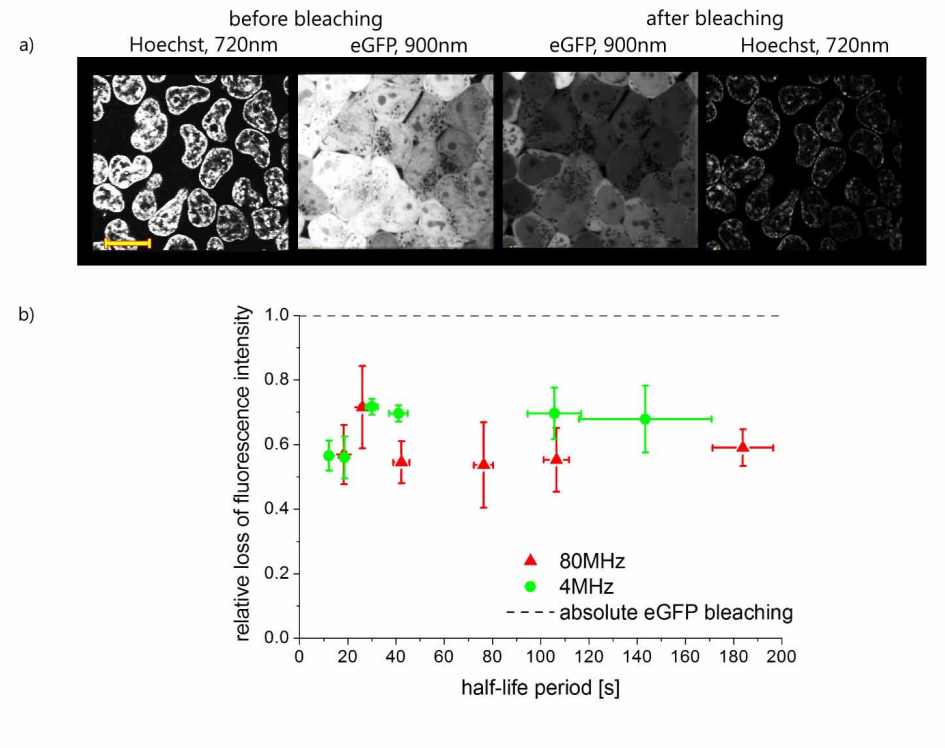

Fig. 6. Influence of eGFP photobleaching on the degradation of Hoechst molecules in its environment. (a) Multiphoton images of Hoechst and eGFP before and after photobleaching of eGFP. Scale bar: 16 μm. (b) Loss of relative Hoechst fluorescence intensity referred to an absolute bleaching of eGFP for different half-life periods and both repetition rates. Each data point represents the mean $\pm$ standard error of at least eight experiments. The loss of Hoechst fluorescence intensity referred to an absolute bleaching of eGFP is within the range of 50-80%.

4. Discussion and conclusion

In this study, we have characterized the high-order photobleaching of the two fluorophores eGFP and Hoechst 33342. For the first time, we examined high-order photobleaching in a large wavelength range and made a comparison to another laser-mediated process in microscopy: intracellular ablation.

The measurements of the multiphoton-order yielded values of approximately two for eGFP, while it increased from two to three with the wavelength for Hoechst (see Fig. 2). Our findings for Hoechst are in agreement with Gryczynski et al. [24]. For eGFP, our results correspond to the large two-photon action cross-section [25] over the whole measured wavelength range.

#141169 - $15.00 USD Received 14 Jan 2011; revised 18 Feb 2011; accepted 20 Feb 2011; published 4 Mar 2011

The photobleaching-order measurements were independent of the repetition rate and NA for both fluorophores (see Fig. 3). Chen et al. found similar data, concerning the NA, for a mutant of the fluorophore GFP [11]. Therefore, diffusion processes in the milli- and microsecond regime, as in the reaction with molecular oxygen, should be negligible in high-order photobleaching, as reported by Dittrich et al. [14]. Our results underline their thesis, that triplet population does not play a key role in high-order photobleaching.

We observed that for normalized fluorescence intensity, the half-life period depended on the wavelength. It increased with the two-photon action cross-section of both fluorophores (data not shown). If photobleaching occurs from the first excited singlet state, the half-life period should be independent of the wavelength [10]. Therefore, we suggest that bleaching of eGFP and Hoechst occurs from a highly excited state or the ground state.

Our results indicate that eGFP bleaching is dominated by multiphoton-ionization of the fluorophore from ground state. The ionization threshold of the eGFP chromophore is in the range of 4.6 to 6.2 eV [26]. This could be reached by a quasi-simultaneous absorption of three or four photons (compare with photobleaching-orders in Fig. 3), but not with a two-photon excitation in the first singlet (2,6 eV [27]) followed by further sequential-absorptions in higher states. This is underlined by the fact that eGFP is likely missing any relevant states far above the first singlet [27]. Therefore, high-order photobleaching of eGFP is independent from two-photon excitation. The step increase in the photobleaching-order at a wavelength of approximately 840 nm can be explained by the multiphoton-ionization of a tryptophan residue 13 to 15 $\AA$ [28] next to the eGFP chromophore. Its ionization energy is 4.5 eV [29], corresponding to the measured transition wavelength of 840 nm divided by the number of interacting photons. This leads to the production of a hydroxyl radical or a free electron [30] and therefore to bleaching by chemical deconstruction. Hence, bleaching is mediated by multiphoton-ionization of the chromophore itself and the tryptophan residue. As multiphoton-ionization becomes less effective with increasing wavelength, the concurrent rise of the half-life period can be well explained.

A study by Bourgeois et al. [31] suggests that the intracellular ablation threshold also has a cubic dependence on excitation power for GFP at a wavelength of 720 nm. For this reason we conclude, that high-order photobleaching as well as ablation of eGFP involves three or four photons and occurs via multiphoton-ionization from ground state. Furthermore, both processes provide free electrons.

We presume that our findings for the photobleaching-order of Hoechst (see Fig. 4) are closely related to a two-photon excitation in the first singlet followed by several sequential-absorption events in higher states. In contrast to eGFP, Hoechst has electronic states above the first singlet [32] in which another one-photon absorption is likely because of the very large photon density [8]. Bleaching is then evoked by one or more one-photon absorptions after excitation into the first singlet. These transitions are not counted in photobleaching-order, as they are saturated [8]. This is why our findings for the photobleaching-order of Hoechst are similar to the ones for the multiphoton-order (compare Figs. 2 and 4). By reaching the ionic state (5.5 eV [33]) or a highly excited state, the Hoechst fluorophore forms an electron-cation pair, which can split up in a polar environment [13]. Kuetemeyer et al. reported ablation threshold dependencies on the fourth and fifth order of laser power at 720 and 950 nm for Hoechst-stained biomolecules, respectively [22]. As ablation is mediated by multiphoton-ionization, we can conclude that the same amount of photons is involved (see Fig. 7) and free electrons are provided in both processes.

If we take into account the formation of free electrons, we have to point out that high-order photobleaching likely produces a low-density plasma [16]. This is quite similar to ablation. By observing a linear dependence of the half-life period on multiphoton image-size (data not shown), we found that high-order photobleaching is also an accumulation of single-pulse

#141169 - $15.00 USD Received 14 Jan 2011; revised 18 Feb 2011; accepted 20 Feb 2011; published 4 Mar 2011

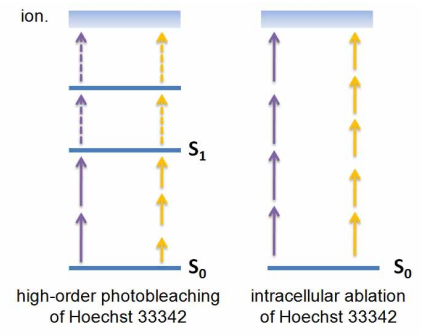

Fig. 7. Schematic of high-order photobleaching and ablation of Hoechst molecules. Violet arrows correspond to wavelengths from 720 up to 920 nm, yellow arrows to 920 nm and above. In photobleaching two or three photons evoke the excitation of Hoechst and another two photons are sequentially absorbed in saturated one photon transitions, while in ablation multiphoton-ionization occurs by the quasi-simultaneous absorption of four or five photons.

events [22]. Therefore, we are convinced that there is a smooth transition between high-order photobleaching and ablation.

The augmentation of reactive oxygen species correlating with bleaching over time (see Fig. 5), indicates the formation of a low-density plasma. Reactive oxygen species are produced by the interaction of biomolecules, water or oxygen with free electrons [16]. Thus, the cell gets confronted with oxidative stress, but intracellular radical scavengers like ascorbic acid or glutathione [21] are able to neutralize this, as we found no major effects on cell viability. However, a significant effect of the low-density plasma became obvious in the non-direct bleaching of Hoechst in the eGFP expressing RAT1 cells (see Fig. 6). It likely results from the interaction of free electrons or reactive oxygen species with dye molecules.

According to the literature, a mammalian cell nucleus with a volume of about 100 fl [34] contains about $6 \cdot 10^8$ Hoechst molecules at the used dye concentration [35, 36]. Therefore, the average distance of two Hoechst molecules was $2r_H \approx 7$ nm. A concentration of at least 0.2 μM eGFP molecules is necessary to make eGFP fluorescence stronger than autofluorescence [36]. As eGFP fluorescence was relatively strong in our experiments, we assume that the eGFP concentration was about 1 μM, corresponding to 60,000 molecules in the cell nucleus. Also taking the ratio of relative fluorescence intensity loss $R_{loss} \approx 0.7$ (see Fig. 6) into account, we were able to estimate the interaction range of electrons or ROS with fluorophores, equal to the low-density plasma radius:

$$r_{LDP} \approx \sqrt[3]{r_H^3 \cdot C \cdot R_{loss} \cdot \frac{3}{4\pi}} \tag{1}$$

where C is the ratio between Hoechst and GFP molecules in the nucleus. The low-density plasma radius was calculated to be in the range of 30 to 50 nm corresponding well to the diffusion length of singlet oxygen being less than 50 nm [36] in cells. As the low-density plasma influences fluorophore-molecules, it is possible that biomolecules were attacked, too. This issue needs further investigations.

To conclude, we have shown that high-order photobleaching is quite similar to ablation. Both processes are equal regarding the amount of involved photons and the accumulation of single-pulse events. High-order photobleaching, however, is mediated by sequential-absorption and multiphoton-ionization, while ablation is dominated by the latter and additionally occurring cascade-ionization processes. For this reason, the involved energetic states are not always

#141169 - $15.00 USD Received 14 Jan 2011; revised 18 Feb 2011; accepted 20 Feb 2011; published 4 Mar 2011

the same. We propose that there are smooth transitions between laser-mediated processes in the low-density plasma regime. This comprises the transitions from sequential-absorption to multiphoton-ionization and finally cascade-ionization, both depending on the fluorophores and biomolecules as the major source for free electrons.

Acknowledgements

This work is supported by funding from the Deutsche Forschungsgemeinschaft (DFG, German Research Foundation) within the Cluster of Excellence *"REBIRTH"* (From Regenerative Biology to Reconstructive Therapy).

#141169 - $15.00 USD Received 14 Jan 2011; revised 18 Feb 2011; accepted 20 Feb 2011; published 4 Mar 2011